SLAC-PUB-16324
May 2015

MICROBUNCHING PHENOMENA IN LCLS-II *

M. Venturini†, J. Qiang, C. Papadopoulos
LBNL, Berkeley, CA 94720 USA
Y. Ding, P. Emma, Z. Huang, G. Marcus, A. Marinelli, Y. Nosochkov, T. Raubenheimer,
L. Wang, M. Woodley
SLAC, Menlo Park, CA 94025 USA

Abstract

The microbunching instability has long been recognized as a potential limiting factor to the performance of X-ray FELs. It is of particular relevance in LCLS-II [1] due, in part, to a layout that includes a long bypass beamline between the Linac and the undulators. Here we focus on two aspects of the instability that highlight the importance of 3D effects.

ANOMALOUS HEATING

'Trickle' Heating

The Laser Heater (LH) is the established method to control the microbunching instability, exploiting the microbunching sensitivity to energy-spread induced mixing. In LCLS-II the LH is located at the exit of the injector at about 100 MeV beam energy; it consists of a 0.54 m undulator placed in the middle of a weak 4-dipole chicane and a $\lambda_L = 1030$ nm laser system. Concerns about the 'trickle' heating effect, discovered during LCLS commissioning [2], motivated the high-resolution numerical studies with the code IMPACT [3] presented here. Trickle heating is an echo-like phenomenon, in which the E/z micro-correlations generated by the laser/electrons interaction in a finite-dispersion region induce z/x correlations on the same micro-scale downstream of the LH (while the E/z micro-correlations are eventually washed out by the finite transverse emittance). The z/x correlations appear at relatively well localized points along the lattice separated by π phase advance in the horizontal betatron motion. The associated longitudinal space-charge forces modify the electron energy resulting into anomalous heating, which is undesirable, as it may compromise accurate control of the heater operation. To speed up the numerical calculations without sacrificing accuracy, we simulate a flat-top bunchlet meant to model a short section of the bunch core (but long enough to span many laser wavelengths). For the $Q = 100$ pC bunches discussed here the peak current in the core is $I_{\rm pk} \simeq 14$ A. For high fidelity simulations, the particle charge is the same as that of a physical electron (this is the case for the results of all the simulations presented in this paper). We track the bunchlet with initial gaussian energy density and σ_{E0} slice rms energy spread, starting from the exit of the injector, a few meters upstream of the LH chicane; σ_{E0} from high brightness injectors is not known very well but is expect to be on the order of 1-2 keV, including IBS effects: in our simulations we exercised a range of values. The action of the laser on the beam is modeled as a point-like interaction inducing a sinusoidal energy modulation and occurring in the middle of the physical undulator. The electron dynamics through the undulator itself is modeled as that of a drift (IMPACT has the capability to track the electrons through the undulator and laser-pulse fields, but it is time consuming and unnecessary for our purposes here). The bunch is followed through the LH chicane and a 50-m long collimation section to the entrance of the first Linac section (L1). An example of bunchlet longitudinal phase space is shown in Fig. 1, left picture. The prominent energy chirp, due to longitudinal space charge in the short bunchlet, is removed in the analysis before determining the energy spread distribution shown in the right picture. For comparison, the density observed at the exit of the LH chi-

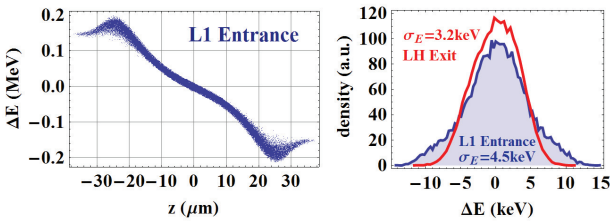

Figure 1: Longitudinal phase-space (left) of bunchlet at entrance of L1 and energy density in the core (right, blue curve). For comparison, the red curve on the right figure is the energy density at exit of the LH chicane;$\sigma_{E0} = 2$ keV.

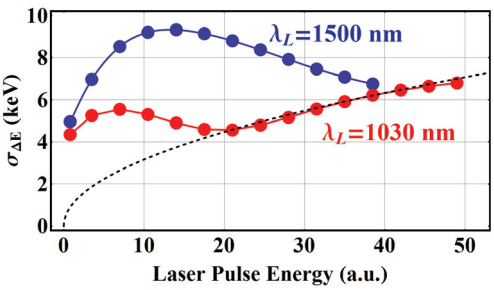

Figure 2: Energy spread at the entrance of L1 (two choices of laser wavelengths) showing evidence of the 'trickle' heating effect; $\sigma_E = 0.1$ keV. The dashed line is the nominal heating in the absence of collective effects.

* Work supported by DOE, in part under Contract No. DE-AC02-05CH11231 and through the LCLS-II project.
† mventurini@lbl.gov

Presented at the 6th International Particle Accelerator Conference (IPAC 2015)
Richmond, VA, USA May 3-8, 2015

This material is based upon work supported by the U.S. Department of Energy, Office of Science, Office of Basic Energy Sciences, under Contract No. DE-AC02-76SF00515.

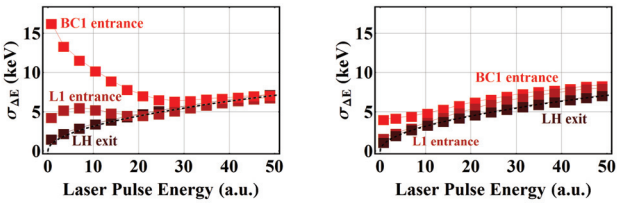

Figure 3: Slice energy spread as observed at the exit of the LH chicane, entrance of L1, and entrance of bunch compressor for a 4 m (left) and 8 m long (right; baseline design) LH chicane, showing evidence of shot-noise induced heating.

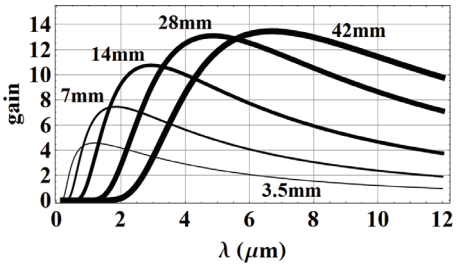

Figure 4: Linear gain curve of the microbunching instability through the LH chicane for several choices of $|R_{56}|$ as indicated. (Constant $\sigma_E = 2.5$ keV through the chicane.)

cane (red curve) is also shown: the difference between the two is (mostly) a consequence of the trickle heating effect. The results of a systematic study, shown in Fig. 2, include data points obtained with $\lambda_L = 1500$ nm (blue dots), longer than nominal, to illustrate the dependence of trickle heating on the laser wavelength. The black-dashed curve is the nominal rms energy spread $\sigma_{\Delta E} \propto \sqrt{E_L}$ induced by the LH as a function of the laser pulse energy E_L (normalized units). Anomalous heating is apparent for small E_L but remains comfortably below the $\sim$ 7 keV threshold believed to be necessary for damping the microbunching instability along the machine. The data points follow a behavior qualitatively consistent with the analytical model discussed in [2]. Notice that in the limit of vanishing laser pulse energy, the observed energy spread does not converge to the energy spread of the incoming beam (in these simulations a negligible $\sigma_{E0} \simeq 0.1$ keV). This is explained in the next section. The above results are for the now outdated design of a 4 m long LH chicane with $|R_{56}| = 14$ mm.

Shot-Noise Induced Heating

Another source of anomalous heating is the microbunching instability induced by shot noise that develops through the LH chicane. The linear gain of the instability is relatively modest but it may be sufficient for longitudinal space charge in the long section between LH chicane and first magnetic compressor BC1 to cause a few keV amplitude energy-modulation. Strictly speaking, this is a correlated energy spread (with E/z correlations on the μm scale). However, as the beam experiences the large R_{56} in BC1 the microcorrelation is flattened causing the energy spread to become effectively uncorrelated. Evidence of enhanced heating is shown on the left picture of Fig. 3 in the (top) data points for the energy spread observed at the entrance of BC1: for low laser pulse energy, the energy spread is significantly larger than that observed at the entrance of L1 (the latter is for the most part dominated by the trickle heating effect). The data points at the exit of the LH chicane track the nominal heating closely, as expected. The reported energy spread is calculated over a distance within the beam that encompasses several wavelengths of the dominant energy modulation. Again, this unintended heating is undesirable as it may compromise the ability to tune the LH and set a lower bound to the minimum beam energy spread. The effect is also difficult to predict accurately because of a strong dependence on the not very well-known slice energy spread at the exit of the injector. In addition, there may be contributions to the microbunching instability from the gun and injector (not captured here), also not easy to predict accurately. It is therefore wise to adopt a lattice design strategy aiming at reducing microbunching amplification through the LH chicane. The instability is sensitive to the choice of R_{56} in the chicane, a variable over which the lattice designer has some degree of control. All the other relevant parameters kept fixed, there tend to be a value of $|R_{56}|$ that maximizes microbunching. Given the relatively small value of the slice energy spread involved, linear theory shows that here decreasing, rather than increasing, $|R_{56}|$ is the more effective way to reduce the instability. This can be seen from the basic scaling predicted by a (simplified) linear-theory model of the instability; see Fig. 4, where the gain curves of the microbunching gain through the LH chicane are reported for various R_{56}. The model is not very accurate (the beam slice energy spread is assumed to have an effective value remaining unchanged through the chicane) but gives a good sense of the scaling involved. We redesigned the chicane to decrease $|R_{56}|$ to 3.5 mm. In order to keep the trajectory offset unchanged at 7.5 cm this was achieved by lengthening the chicane to 8 m while reducing the bend angle in the dipoles. Overall, anomalous heating in the presence of the modified chicane is much reduced (right picture in Fig. 3). Both pictures in Fig. 3 were obtained with a conservative choice for the beam natural slice energy spread out of the injector ($\sigma_{E0} = 0.1$ keV).

TRANSVERSE SPACE-CHARGE (TSC) INDUCED MICROBUNCHING

A somewhat surprising finding of our study was the discovery of a new mechanism for the amplification of microbunching, driven by the transverse rather than the longitudinal component of the self-fields as one would normally expect. We first observed this effect while investigating the beam dynamics through first dogleg (DL1) past the Linac, which takes the beam into a long bypass above a portion of the existing Copper machine toward the spreader

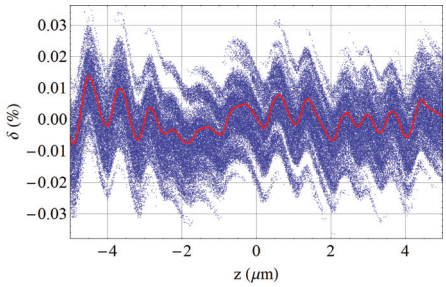

Figure 5: Longitudinal phase space of the beam core at the entrance of DL1. The red curve is the slice centroid energy. The apparent $\sim$ 1 μm energy modulation is the result of longitudinal space charge during acceleration and transport following the second bunch compressor, placed about 700 m upstream of DL1.

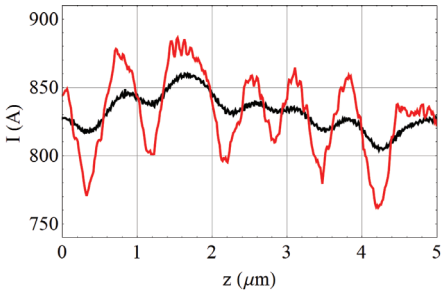

Figure 7: The beam current profile as seen at the entrance of DL1 (black curve) shows $\sim$ 1% longitudinal bunching amplitude at about $\lambda \simeq 1$ μm wavelength. By the exit of the dogleg (red curve) bunching has grown to about 4%, implying a net $\sim$ 3% contribution from TSC in the dogleg. The quoted numbers are about the middle of the observed value ranges.

and the undulator hall. The effect occurs in the presence of imperfect damping of the the microbunching instability through BC2; for 100 pC bunches this is the case for the nominal 7 keV settings of the laser heater. This leaves a few % microbunching on the beam at $\lambda \simeq 1$ μm at the exit of BC2 (coincidentally the same as the LH laser wavelength), which by the entrance to the dogleg results into a non-negligible energy modulation, see Fig. 5. The dogleg in the baseline design is about 80 m long and is delimited by two $\sim$ 1 m long dipoles with 25 mrad bend angle. We recognized early on that the dogleg could trigger a 'conventional' (*i.e.* through the longitudinal component of the space-charge self-fields) amplification of the microbunching instability [4] and suggested use of small 4-dipole compensating chicanes placed next to the dogleg bends to provide local $|R_{56}|$ compensation; we also recognized that a non-negligible 2$^{\rm nd}$-order momentum compaction T_{566} in combination with finite beam energy chirp would be problematic (more on this will be reported elsewhere). Yet, when provisions were taken to eliminate these effects from the simulations we determined that a small but significant enhancement of bunching continued to persist, caused by transverse space-charge forces within the dogleg. The mechanism is somewhat reminiscent of the trickle

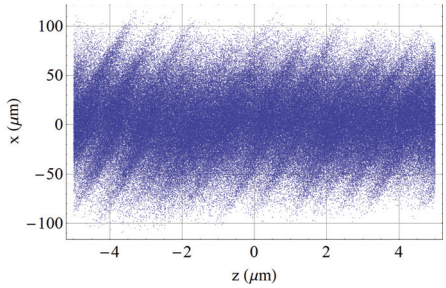

Figure 6: Section x/z of the beam phase space observed just before the first quad of the dogleg showing the longitudinal/transverse microbunching induced by the energy modulation of Fig. 5.

heating effect: in both cases an energy modulation couples with dispersion to cause the appearance of a 2D longitudinal/horizontal pattern in the beam density on the scale of the energy modulation wavelength at certain locations within the dogleg, see Fig. 6. The transverse component of the space charge associated with this pattern kicks the beam particle horizonal angular coordinate by $\Delta x'$. Because the matrix entry R_{52} from location of the kick to exit of the dogleg is generally finite, a longitudinal shift is induced, $\Delta z = R_{52}\Delta x'$, enhancing the existing bunching, as observed at the exit of the dogleg, Fig. 7. One can show that under certain simplifying assumptions discussed in [5] the additional bunching can be expressed in the form

$$b_k \simeq \delta_p \frac{2Ik}{\varepsilon_{xn}\gamma^2 I_A}\int_{s_0}^{s_f} ds \frac{\eta_x^2}{\sqrt{\beta_x\beta_y}} e^{-\frac{\varepsilon_{xn}\eta_x^2 k^2}{\gamma\beta_x}},$$

where δ_p is the relative energy-modulation amplitude at the entrance of the dogleg with wavenumber k and the notation for the various quantities follows standard conventions ($I = 850$ A, $\varepsilon_{xn} = 0.3$ μm, $mc^2\gamma = 4$ GeV). The integral is over the dogleg length and the expression is valid under the assumption that R_{56} is locally compensated. The formula agrees reasonably well with the results of the numerical simulations. The gain through dogleg is small but not insignificant, and it can be compounded by further amplification of the microbunching instability in the downstream section of the machine (which includes the long bypass section, a spreader, and additional dispersive transport lines to the hard and soft x-ray FELs). A more comprehensive analysis will be reported elsewhere.

REFERENCES

[1] J. Galayda, IPAC 2014, Dresden, Proc. p. 935 (2014).

[2] Z. Huang, *et al.*, PRST-AB **11**, 020703 (2010).

[3] J. Qiang, *et al.*, PRST-AB **12**, 100702 (2009).

[4] M. Venturini and A. Zholents, NIM-A **539**, 53 (2008).

[5] M. Venturini and J. Qiang, to appear in PRST-AB (2015).